https://doi.org/10.5194/acp-2022-452
Preprint. Discussion started: 12 July 2022

Atmospheric Chemistry and Physics Discussions

High accuracy calculation and data quality evaluation of ship emissions based on the sniffer method

Letian Zhu[1,2], Fan Zhou[1,2]

[1]College of Information Engineering, Shanghai Maritime University, Shanghai 201306, China
[2]Shanghai Engineering Research Center of Ship Exhaust Intelligent Monitoring, Shanghai 201306, China

Correspondence to: Fan Zhou (fanzhou_cv@163.com)

Abstract. More attention has been paid to the air pollution caused by ship emissions; hence the establishment of accurate emission inventories is an important means to assess the impact on the environment and human beings. The emission factor is an important parameter in the process of compiling the ship emission inventory, yet there is some uncertainty in its estimation based on the sniffer method. In this study, taking the calculation of SO_2 emission factors as an example and aiming at the selection of gas measurement values using the sniffer method, the concept of standard deviation of peak density was proposed to determine the optimal integral interval length of the measured values of SO_2 and CO_2. Then, the improved Manhattan distance was used to characterize the position of the peak points in the SO_2 and CO_2 average series. Using the dynamic time warping algorithm, the corresponding relationship of the peak points in the average series of the measured gases was determined, and the global optimal peak points were selected from it. To evaluate the credibility of calculated emission factors, 16 evaluation indexes that reflect the characteristics of the measured data were selected. The confidence interval of 95% of each evaluation index was calculated using self-development sampling of the measured data, and the evaluation result of the evaluation index for the quality of the measured data was obtained. Combined with the data quality label, the indexes with high correct rate were screened. Finally, the evaluation scores were determined according to these selected indexes. We collected a total of 148 sets of "SO_2+CO_2" measurement data between 2019 and 2021 using the unmanned aerial vehicle sniffing monitoring system in the Waigaoqiao Port area of Shanghai, China for verification using the method proposed in this study. The results show that for this data set, 12 s is the most suitable integral length, with which the algorithm can automatically calculate the emission factor. The screening results of the global optimal peak points of 129 groups of data are consistent with those of artificial screening, with a correct rate of 87.16%. The accuracy of the combined evaluation of sample entropy (SO_2), information entropy (SO_2), skewness (CO_2) and quartile spacing (SO_2) is 71%. Previous calculation of the emission

https://doi.org/10.5194/acp-2022-452
Preprint. Discussion started: 12 July 2022

Atmospheric Chemistry and Physics Discussions

factor of ships mainly focused on different conditions such as time, region, fuel, engine, ship type, and navigation status. Our in-depth study proposes a high accuracy ship emission factors calculation method and an evaluation of the quality of the measurement data that reduces uncertainty in the current sniffer technique monitoring ship emission research.

1 Introduction

In the past decade, the development of the global shipping industry has accelerated (UNCTAD, 2021), resulting in increasingly serious emission problems (Chen et al., 2019). Gases and particles emitted by ships will not only pollute the natural environment, but also have an impact on human health (Liu et al., 2016). SO_2 causes frequent acid rain damage to the environment (Matthias et al., 2010) such as the erosion caused to 50% and 30% of the forests in Germany and Poland and Switzerland, respectively (Mohajan et al., 2018). Fine particulate matter ($PM_{2.5}$) can cause lung cancer and other heart and lung diseases, and results in 2.2 million to 3.3 million deaths worldwide each year (Sofiev et al., 2018). In 2015, a total of 20.1×10^6 tons of NO_x, 11.5×10^6 tons of SO_x, and 1.54×10^6 tons of PM were emitted by global shipping operations (Sofiev et al., 2018). In 2017, EU shipping emissions generated 2.6×10^6 tons of SO_2 and 7.7×10^6 tons of NO_2 (Jonson et al., 2020).

Accurate ship emission inventory is not only the baseline data for analyzing the law of ship emissions, but also the scientific basis for controlling and optimizing supervision measures in relevant management areas (Zhang et al., 2017; Zhang et al., 2017). The calculation of ship emission inventory is carried out using two approaches: top-down and bottom-up. The top-down method is based on the fuel consumption of the ship without considering its specific location, and is suitable for the calculation of the long-term source list on the global scale. Kesgin et al. (2001) used the top-down method to calculate the emissions of CO, CO_2, $PM_{2.5}$ from ships in the Turkish Strait. Corbett et al. (1997) studied the global emission inventory using ship fuel. The bottom-up method directly estimates emissions based on the motion state and attributes of the ship, which is more accurate than the top-down method. In recent years, due to the rapid development of the Automatic Identification System (AIS), it is more convenient to obtain the real-time operation status of ships, hence this method is widely used in the research of emission inventory. Papaefthimiou et al. (2016) used a bottom-up approach based on port ship activity to calculate the NO_x, SO_2, $PM_{2.5}$ emitted by international cruise ships in 18 ports in Greece. Tichavska et al. (2015) obtained

https://doi.org/10.5194/acp-2022-452
Preprint. Discussion started: 12 July 2022

Atmospheric Chemistry and Physics Discussions

ship activity data through the AIS and studied the monthly relationship between ship emissions and vessel type in Las Palmas Port.

Parameter information such as ship speed and position, main engine power, auxiliary power, and emission factors are needed when establishing an emission list. Among them, the static and dynamic information of the ship can be obtained directly using AIS data and other channels, whereas the emission factor can only be determined by measurement, thus the accuracy of the measurement directly determines the accuracy of the emission list (Ekmekçioğlu et al., 2020; Yang et al., 2021; Toscano et al., 2021). There are two ways to measure emission factors: fuel- and power-based. The former can be calculated by measuring the concentration of CO_2 and other pollutants, while the latter needs to obtain real-time data of mainframe power, auxiliary power, and operation mode. The two measurements can be converted to each other when the ship fuel consumption rate is known (Zhang et al., 2016). Sniffer technique is one of the methods based on the fuel emission factor measurement, which can quickly and accurately calculate the ship plume. Balzani Lööv et al. (2014) used the sniffer technique among others to compare the measures of the emission factor and fuel oil sulfur content of ships in the port of Rotterdam. The mobile sniffer technique was the most convenient and accurate, with an average random error of 6% for SO_2 emission factors. Beecken et al. (2014) used a small aircraft carrying sniffer equipment to monitor exhaust emissions from 158 ships in the Baltic Sea and North Sea. The average emission factor of SO_2 was $18.8 \pm 6.5 kg_{fuel}^{-1}$, and approximately 85% of the monitored ships met the sulfur content limit set by the International Maritime Organization. Many studies have shown that the emission factor and its accuracy is an important parameter in the compilation of ship emission inventory (Moreno-Gutiérrez et al., 2015; Zhang et al., 2017; Ekmekçioğlu et al., 2020). Therefore, many emission factors measurements have been proposed to obtain accurate results. These experiments focused more on measuring and obtaining emission factors under different conditions such as time, region, fuel, engine, ship type, and navigation status (Sinha et al., 2003; Cooper, 2003; Burgard and Bria, 2016; Peng et al., 2016; Betha et al., 2017; Liu et al., 2018; Bai et al., 2020). However, there is still a lack of in-depth research on how to accurately calculate the emission factor from measurement data and how to evaluate the quality of the measured data.

Taking SO_2 as an example, the principle of the sniffer technique is based on the 85% and 87% stability of the carbon content in ship fuel. The concentration ratio of CO_2 to SO_2 generated by fuel combustion is equal to the molar ratio of carbon to sulfur in the fuel and will not change due to tail gas dilution, thus

https://doi.org/10.5194/acp-2022-452
Preprint. Discussion started: 12 July 2022


Atmospheric Chemistry and Physics Discussions

the measurement of CO_2 and SO_2 concentration can be used to calculate the emission factor (Huang et al., 2021). However, various uncertain factors in the calculation process cause nonnegligible interference to the emission factor, which mainly exists in three aspects: first, because the response time of different gas sensors varies, it is difficult to select the measured value of gas at the same time as the calculated emission factor. Therefore, the general method is to select the gas measurement values for a period for the cumulative calculation to reduce the error caused by the response time of different gas sensors that cannot be synchronized. Zhou et al. (2020) proposed to regard the accumulation process as an integral, and then divide the result by the time interval, so as to convert the gas measurement into an average value to find a method that selects the global optimal peak point of the gas average value. The problem of selecting the appropriate integral interval is selecting the global peak point in the average set of measured data. However, the time interval of the integral interval mainly depends on experience. Second, based on the first problem, the selection of the global optimal peak point directly determines the accuracy of the emission factor calculation. However, multiple peaks of SO_2 and CO_2 will appear in gas measurements over a period. Therefore, there is a lack of in-depth research on how to establish a matching relationship between the peak points to determine the global optimal peaks of SO_2 and CO_2. Third, various environmental and equipment factors in the process of ship exhaust gas measurement will interfere with the gas measurement value, hence there is no objective evaluation method for the gas measurement value at present.

This study makes an in-depth study and analysis of the above three problems. Aiming at the first problem, the concept of peak density standard deviation is proposed to measure the ability of an integral interval to represent the changing data. The larger the value of the standard deviation of peak density, the more obvious the changes of the data processed by the corresponding integral interval, the clearer the peak trend, and the more accurate the selection of the global optimal peak point. Aiming at the second problem, to select the optimal peak point from many peak points, it is necessary to establish a matching relationship between the average series of the two gases and judge the rationality of all the matching relations. The dynamic time warping (DTW) algorithm was proposed by Itakura (Itakura, 1975), and its function is to measure the similarity of two time series. Dmytrów et al. (2021) recently used the DTW algorithm to evaluate the similarity between energy commodity prices and the daily cases time series for the coronavirus disease (COVID-19). Li et al. (2020) used the DTW algorithm to compare the corresponding relationship between ship trajectory time series, which improved the performance of navigation trajectory

https://doi.org/10.5194/acp-2022-452
Preprint. Discussion started: 12 July 2022


Atmospheric Chemistry and Physics Discussions

modeling. Applying the DTW algorithm to the screening of peak points can obtain the similarity between CO_2 and SO_2 sequences and the matching relationship between the average sequences of their peak points. Further, combining the criteria for selecting the optimal peak points proposed by Zhou et al. (2019) can select the appropriate gas measurement value for the calculation of emission factors. Aiming at the third problem, 16 evaluation indexes that reflect the data quality are put forward, in which the evaluation index for a single gas measurement value is divided into two cases to use the SO_2 and CO_2 measurement values for evaluation, respectively. The 95% confidence interval of the evaluation indexes are calculated by self-developing sampling for a number of measured data, and the evaluation results of these indexes for the quality of the measured data are given accordingly. Combined with the quality label of the measured data, the correct rate of the index for data quality evaluation can be obtained, and the evaluation indexes with higher accuracy can be selected to form a set for joint evaluation, so as to further improve the accuracy of the gas measurement data evaluation. Finally, using the method proposed in this study, the ship exhaust data measured in Shanghai Waigaoqiao Port are tested, and it is verified that this method can find the appropriate global optimal peak point with high accuracy and then calculate the emission factor, using indexes to jointly evaluate the quality of the measured data.

2 Theory

2.1 Method of calculating ship emission factors

The sniffer method is based on three assumptions: first, the carbon content in different ship fuels is approximately 87% similar. Second, the combustion of carbon and sulfur in ship fuel produces almost all CO_2 and SO_2, while the rest of sulfur and carbon oxides account for only a small part, which can thus be ignored. Third, when the tail gas generated by marine fuel combustion is diluted in the air, the ratio of CO_2 to SO_2 does not change (Hu et al., 2018). Accordingly, the SO_2 emission factor can be calculated by measuring the gas concentration of SO_2 and CO_2 over a period and accumulating the ratio respectively. The formula is (Beecken et al., 2014):

$$EF_{SO_2}[g\ kg_{fuel}^{-1}] = \frac{m(SO_2)}{m(fuel)} = \frac{M(SO_2)\cdot\sum[SO_{2,ppb}]}{M(C)/0.87\cdot\sum[CO_{2,ppm}]} = 4.64\frac{\sum[SO_{2,ppb}]}{\sum[CO_{2,ppm}]} \quad (1)$$

where $m(\cdot)$ is the mass, $M(C)$ is the relative atomic mass of carbon, $M(SO_2)$ is the relative molecular mass of sulfur dioxide, and $\sum[\cdot]$ is the cumulative summation of the concentration of the gas to be measured over time.

https://doi.org/10.5194/acp-2022-452
Preprint. Discussion started: 12 July 2022

Atmospheric Chemistry and Physics Discussions

Considering that the sensor cannot achieve complete synchronization, the method of accumulating the measured values over a period can be adopted instead of using one measured value, that is, the calculation of the emission factor can be more stable by integrating the measured values of gas over a period. In this study, we calculate the SO_2 emission factor by converting gas measurements into average values, as shown in Eq. (2) (Zhou et al., 2020):

$$EF_{SO_2}\left[g\ kg_{fuel}^{-1}\right] = 4.64\frac{\int(SO_{2,peak}-SO_{2,bkg})dt[ppb]/_t}{\int(CO_{2,peak}-CO_{2,bkg})dt[ppm]/_t} = 4.64\frac{AVG(SO_{2,peak})-AVG(SO_{2,bkg})}{AVG(CO_{2,peak})-AVG(CO_{2,bkg})} \quad (2)$$

where $SO_{2,peak}$ is the peak of SO_2 in the measured data, $SO_{2,bkg}$ is the background value of SO_2 in the measured data, t is the length of the integral interval, $\int(\cdot)dt$ is the integral calculation function of the integral interval of t seconds, and $AVG(\cdot)$ is the function of calculating the average measured value in t seconds.

Using the above transformation, the problem of selecting the integral interval of gas using the sniffer technique is selecting the integral interval and peak point. The empirical value of 10 s was used by Zhou et al. (2020) in the integration interval, and then by observing and analyzing the changing trend of the peak point in the average series, the appropriate global optimal peak point was selected for the calculation of emission factors. Through the above methods, more accurate results can be calculated. However, the length of the selected integral interval belongs to empirical value, which lacks theoretical demonstration. In addition, when there are many peak points in a period, there is also uncertainty about how to pair SO_2 and CO_2.

2.2 Dynamic time warping algorithm

In order to eliminate the inconsistency of response time between SO_2 and CO_2 sensors, it is necessary to find the matching relationship between the peak points on the average sequence of SO_2 and CO_2, so that the global optimal peaks with corresponding relationship can be screened. According to the distance relationship between peak points, this study uses the DTW algorithm to establish the matching relationship between the SO_2 and CO_2 peak points. The purpose of the DTW algorithm is to find the difference between each data point in the target and standard time series, calculate the minimum value after the difference accumulation, and determine the corresponding path, which is used to match the peak points of SO_2 and CO_2 in this study. The target time series is marked as $X = (x_1, x_2, \dots, x_n)$. The standard time series is written as $Y = (y_1, y_2, \dots, y_m)$. In this study, we correspond to the results of peak point

https://doi.org/10.5194/acp-2022-452
Preprint. Discussion started: 12 July 2022

Atmospheric Chemistry and Physics Discussions

extraction from the SO_2 and CO_2 average series. f represents the distance between the points on the target time series and its corresponding standard time series in an unbiased ideal state:

$$d(i,j) = f(x_i, y_j) \tag{3}$$

The distance matrix D is obtained by calculating the distance between the data points and their corresponding points in X and Y:

$$D_{ij} = d(i,j) \tag{4}$$

The shortest distance is to use the cost matrix D_{cost} iteration to calculate the dynamic programing path distance between the target and the standard sequences, and the shortest distance path represents all the matching relations of the data points on the two sequences.

$$D_{cost}(i,j) = D(i,j) + \min\left(D_{cost}(i-1), D_{cost}(j-1), D_{cost}(i-1, j-1)\right) \tag{5}$$

The path corresponding to the shortest distance matrix between the CO_2 and SO_2 peak points is obtained by the DTW algorithm, that is, the matching relationship between the peak points in the SO_2 and CO_2 average sequence is obtained, which can correct the deviation sequence.

3 Method

The high accuracy calculation of emission factors needs to select the measured values of stable air flow over a period and eliminate the influence of various uncertain factors as much as possible. In this study, we first determine the selection method of the optimal integral interval length. Then, use the DTW algorithm to find the matching relationship between the peak points on the CO_2 and SO_2 average series, and select the global optimal peak points. Finally, a quality evaluation method of ship exhaust measurement data is proposed, which is used to evaluate the reliability of the measurement results. The specific process is divided into the following four steps:

1. Selection of integral interval length and extraction of peak points. The concept of standard deviation of peak density is put forward to analyze the distribution law and changing trend of peak points in the measured value sequence, the larger the value of standard deviation of peak density is, the longer the corresponding integral interval can make the calculation of emission factors more stable. The measured value is converted to the average value of the length of the integral interval, and all the peak points in the average sequence are extracted;
2. DTW-based matching. The DTW algorithm based on the improved Manhattan distance is used

https://doi.org/10.5194/acp-2022-452
Preprint. Discussion started: 12 July 2022


Atmospheric Chemistry and Physics Discussions

to correct the average sequence and obtain the matching relationship between SO_2 and CO_2 peak points;

3. Filtering matching relationships. The matching relationship between the peak points in some measured data is established, and all the matching relations are taken as samples for k-means mean clustering. If they can be stably divided into two categories, it shows that the dividing line between the two categories can distinguish between normal and abnormal changes, thus the threshold of concentration change is found. Combined with the time span threshold, the results from step 2 are screened and the abnormal matching results are eliminated. The matching result containing the maximum average value of SO_2 is found among the reserved matching results, and the matching result containing the maximum average value of CO_2 is selected as the global optimal peak point from all the matching results found;

4. Evaluation of measurement data quality. Sixteen evaluation indexes, which can characterize the data quality are proposed. For several measurement data obtained, the 95% confidence interval of each index is calculated by self-expansion sampling. If the index value is in the confidence interval, it is marked as 1, otherwise 0. Combined with the quality label of the measured data, some indexes with strong representation ability are selected from the 16 indexes to form a set of indexes for joint evaluation. The distance between the index value of the measured data and overall mean of the central position of the confidence interval is calculated, and the ratio of the distance to the unilateral length of the confidence interval is obtained (a ratio greater than 1 is reassigned to 1). In joint evaluation, if the calculated ratio of all indexes is 1, the quality of the measured data is judged to be poor; otherwise, the average value of all ratios less than 1 is calculated, and the closer the mean is to 0, the better the quality of the measured data is.

In Section 3.1, the principle and method of selecting the length of integral interval are introduced in detail, and the definition of peak point is explained. Section 3.2 introduces the use of the DTW algorithm to match peak points so as to correct the average sequence of SO_2 and CO_2. At the same time, a distance calculation method based on the Manhattan distance is proposed, which can represent the distance relationship between the peak points in the average sequence. The calculation method of the threshold used to eliminate abnormal matching relations is described in detail in Section 3.3. Section 3.4 describes the specific method of selecting indexes from the 16 evaluation indexes to form an index set for joint evaluation.

https://doi.org/10.5194/acp-2022-452
Preprint. Discussion started: 12 July 2022

Atmospheric Chemistry and Physics Discussions

3.1 Selection of integral interval length and extraction of peak points

When sniffer equipment is used to monitor the ship exhaust, because the response time of SO_2 and CO_2 sensors cannot be completely synchronized, there is a deviation between the time series of CO_2 and SO_2 measurements. Using the appropriate integral interval length (set to t) to convert the measured value per second into the average value within t seconds can reduce the deviation between time series to a certain extent.

However, setting t often adopts an empirical value, which is not supported by theoretical basis generating great uncertainty. If the selected t value is too small, there will be too many small peaks in the overall measurement data set, or a peak composed of multiple data points, which causes great difficulties in the selection of peak values, resulting in great instability in the calculation of emission factors. On the other hand, if the selected t value is too large, the fluctuation of the whole data set is relatively smooth, which cannot show a representative peak trend, which will hinder the selection of the peak value and have a great impact on the calculation of emission factors.

This study proposes a method to determine the optimal integral interval from the point of view of data mining, to reduce the uncertainty of artificial selection of empirical values. To select a suitable integral interval for preprocessing, it is necessary to analyze multiple alternative intervals, because the peak points need to be composed of at least three data points, and very large intervals will excessively smooth the data change trend. Therefore, we only need to find the corresponding relationship between the data change trend and interval, thus the selection range of the integral interval length is from 3 s to 30 s. The sliding window algorithm is used to traverse the measured values, with the window size representing the length of the alternative integral interval; the window moves one point at a time, and the ratio of the peak points of each window to the total data points of the window is calculated. The ratio is the peak density of the window, and the peak density standard deviation of the length of the alternative integral interval is calculated to reflect its changing trend in the measured value. Comparing the peak density standard deviation of each alternative integral interval length, the larger the value, the more the length of the integral interval can reflect the fluctuation of the peak density in the measured value. The specific steps of this method are as follows:

1. Assuming that there are n measurements in a complete measurement process, the sliding window algorithm is used to traverse all the measurements. The window size is the length of the selected integral interval, and the window moves one measured value each time;

https://doi.org/10.5194/acp-2022-452
Preprint. Discussion started: 12 July 2022

Atmospheric Chemistry and Physics Discussions

2. If a measurement point is larger than the left and right adjacent measurement points, the point is defined as the peak point. The number of peak points in each window is calculated, and the peak density of the window is calculated following Eq. (6).

$$density(j) = \frac{count_{peak(j)}}{count_{data(j)}} \quad (6)$$

where $density(j)$ represents the peak density of the j window, $count_{peak(j)}$ represents the number of peak points of the j window, and $count_{data(j)}$ represents the total number of measurement points of the j window;

3. The peak density standard deviation of all windows is calculated during this period of measurement;

$$s = \sqrt{\frac{\sum_{j=1}^{n}(density(j) - average_{density})^2}{n-1}} \quad (7)$$

4. If there are N segments of complete measurement process, steps 1-3 are performed to get a total of N peak density standard deviations, and the mean is calculated;
5. The alternative integral interval length of 3–30 s is used to perform steps 1–4 respectively, and the maximum integral interval length is the optimal integral interval length.

Using the optimal integral interval length, the measured sequence of SO_2 and CO_2 is transformed into the average sequence of SO_2 and CO_2 respectively according to Eq. (2), and all the peak points in the sequence are extracted for subsequent matching.

3.2 Matching based on DTW

The concentration of SO_2 in the ship plume is generally 0–10 ppm. The concentration of CO_2 and SO_2 are not in the same order of magnitude of 300–10000 ppm. For these to match using the DTW algorithm, the average sequences of SO_2 and CO_2 need to be normalized by 0–1 to obtain new SO_2 and CO_2 sequences (marked Q and C):

$$Q = \left\{\frac{SO_2data(i) - SO_2data(min)}{SO_2data(max) - SO_2data(min)}\right\} \quad i = 1,2,\dots,n \quad (8)$$

$$C = \left\{\frac{CO_2data(i) - CO_2data(min)}{CO_2data(max) - CO_2data(min)}\right\} \quad j = 1,2,\dots,n \quad (9)$$

The DTW algorithm calculates the similarity based on the Euclidean distance matrix between two sequences. In the calculation of the Euclidean distance, only one-dimensional numerical value is considered, whereas the selection of the global optimal peak point needs to consider not only the relative size of the concentration, and the time span (the response time deviation of different sensors is usually a few seconds). The matching between two points with a large time span belongs to abnormal matching, so it is necessary to use two-dimensional the relative position relationship to represent the distance between two points. The Manhattan distance considers the values on the two axes, which is more suitable

https://doi.org/10.5194/acp-2022-452
Preprint. Discussion started: 12 July 2022

Atmospheric Chemistry and Physics Discussions

for the selection of the global optimal peak point than the Euclidean distance. Because the average value has been normalized, the time span needs to be converted to a value between 0 and 1, so it is replaced by the ratio of the time span to the total sequence length:

$$d(Q_i, C_j) = \frac{|i-j|}{n} + |y_i - y_j| \tag{10}$$

In the Manhattan distance calculated following Eq. (10), the proportion of $|y_i - y_j|$ is too large, thus we add a compensation coefficient to balance the size of the two dimensions:

$$d(Q_i, C_j) = \frac{|i-j|}{n} * 9 + |y_i - y_j| \tag{11}$$

Through the improved Manhattan distance, a distance matrix of $k * m$ is constructed (the number of SO_2 and CO_2 peak points is k and m, respectively), which is marked as A, in which the point (i, j) represents the distance $d(Q_i, C_j)$ between the i point of Q and the j point of C. The smaller the $d(Q_i, C_j)$ value, the higher the similarity between Q_i and C_j. Finding a warping path in the matrix A starts from the $(0,0)$ point of the matrix to the end of the (k, m) point, and the superposition produces the smallest distance. The warping path is mainly constrained by the following three aspects: monotonicity, continuity, and boundary conditions.

1. The monotonicity constraint means that the warping path can only extend in the prescribed direction. For a point (a, b) on the path and the next point (a', b') on the path, it must satisfy $0 \leq (a' - a)$ and $0 \leq (b' - b)$;
2. The constraint of continuity means that any point in sequence Q and sequence C can be mapped in a warping path, which can only be aligned adjacent to each other and not matched across points. For a point (a, b) and the next point (a', b') on the path, it must satisfy $(a' - a) \leq 1$ and $(b' - b) \leq 1$;
3. The constraint of the boundary condition means that the first and last point on the warping path must be $(0,0)$ and (k, m).

Starting from $(0,0)$, each point in the sequence Q and C is matched one by one, and the distance is accumulated. When the final cumulative distance is reached (k, m), the result is the final distance measure of the sequence Q and C, that is, the similarity between Q and C. Recursion can be performed following Eq. (12):

$$\psi(i, j) = d(Q_i, C_j) + min\begin{cases} \psi(i, j-1) \\ \psi(i-1, j-1) \\ \psi(i-1, j) \end{cases} \tag{12}$$

Each point on the warping path corresponds to a SO_2 and CO_2 peak points, with a matching relationship between the two points. However, some of the peak points extracted from the average series are due to

https://doi.org/10.5194/acp-2022-452
Preprint. Discussion started: 12 July 2022


Atmospheric Chemistry and Physics Discussions

small fluctuations caused by the interference of external environmental factors during the measurement, which will affect the direction of the warping path when participating in the match. Therefore, the matching results are not all reasonable, and this is what needs to be selected.

3.3 Filter matching relationship

The points of the warping path found by the DTW algorithm in the distance matrix do not have a reasonable matching relationship. Zhou et al. (2019) previously proposed several criteria to be followed when selecting the global optimal peak point: one is to eliminate the sharp changes of the peak point, because these abnormal changes are caused by the uncertainty of the sensor, the monitored gas and its content in the atmosphere will affect the selection of the global optimal peak point; the other is to eliminate the peak point with a time span of more than 20 s.

In a completely ideal case, the average sequence of SO_2 and CO_2 should be in a state of complete synchronization. When the monitoring equipment slowly approaches the plume of the ship, the average value of SO_2 and CO_2 will increase, but when it is far away from the plume, it will be in a decreasing trend. Because the ideal state will not be disturbed by external environmental factors or the sensor itself, at any time, the average difference between SO_2 and CO_2 will remain stable and will not change greatly. However, in the actual measurement, the complex external environment may make the average difference at different time points different, hence it cannot be used as the global optimal peak point. Therefore, it is necessary to find a threshold that can distinguish between normal and abnormal changes, and eliminate the matching results with a large difference in average. In this study, the K-means clustering algorithm is used to cluster the difference of the normalized mean of all matching results (marked as D) and obtain the threshold to distinguish between normal and abnormal changes. The specific process is as follows:

1. The number of initial cluster centers k is 2, that is, the sample set is divided into two categories, normal and abnormal changes;
2. Two data points in D are randomly selected as the initial cluster centers of the two clusters;
3. The similarity between each sample point and the two cluster centers is calculated, and the sample points are divided into the clusters corresponding to the cluster centers with the greatest similarity;
4. The cluster center of each cluster is recalculated based on the samples in the existing cluster;
5. Iteration through steps 3 and 4 is performed until the center of the cluster no longer changes.

After multiple k-means clustering of D, if D can be stably divided into two categories, then the threshold has been found. If the normalized difference of SO_2 and CO_2 in the matching result is greater than the

https://doi.org/10.5194/acp-2022-452
Preprint. Discussion started: 12 July 2022

Atmospheric Chemistry and Physics Discussions

threshold, it shows that the matching result belongs to abnormal change and should be eliminated. According to the above two conditions, the reasonable matching results are screened out, and those containing the maximum average value of SO_2 are retained, while the matching results containing the maximum average value of CO_2 are selected as the global optimal peak point from all the matching results found.

3.4 Evaluation of measurement data quality

Using the above methods, the automatic calculation of emission factors can be realized. However, there is no suitable method to evaluate the quality of the measured data. Therefore, this study proposes a method to evaluate the quality of the measured data, according to the index calculation results of the measured data. In this study, 16 evaluation indexes are proposed, which are sample entropy, information entropy, third quartile, standard deviation, skewness, standard deviation of peak density, permutation entropy, fuzzy entropy, approximate entropy, mutual information, first quartile, kurtosis, DTW shortest distance, quartile spacing, coefficient of variation, and ratio of the number of peak points. Among them, the shortest distance of DTW, the ratio of the number of peak points, and mutual information are obtained by calculating SO_2 and CO_2 measurement data. The rest of the evaluation indexes can be obtained only by calculating SO_2 or CO_2. To ensure the accuracy of the evaluation results, for these indexes, we need to use SO_2 and CO_2 measurement data, and select the set with higher accuracy to calculate the index. The role of each evaluation index is shown in Table 1.

Table 1: Sixteen evaluation indexes and their roles in evaluating data quality.

Evaluation index name	Role
Sample entropy **Information entropy** **Permutation entropy** **Fuzzy entropy** **Approximate entropy**	Evaluating the random degree of the sequence can be used to study whether the complexity of the measured sequence is related to the selection of peak points.
DTW shortest distance **Mutual information**	Measure the relationship between multiple sequences.
Ratio of the number of peak points	Measure the relationship between the difference in the

https://doi.org/10.5194/acp-2022-452
Preprint. Discussion started: 12 July 2022

Atmospheric Chemistry and Physics Discussions

	number of peak points in a series and the results of global optimal peak point screening.
Standard deviation of peak density	Reflect the aggregation trend and data change trend of peak points in the series.
First quartile **Third quartile** **Quartile spacing**	Reflect the distribution law of measured values.
Skewness	Measure the asymmetry of the sequence distribution.
Kurtosis	Measure the steepness of the sequence distribution.
Standard deviation **Coefficient of variation**	Measure the degree of dispersion of the sequence as a whole.

The uncertainty of the evaluation index can be quantified using the numerical method based on self-expanding sampling, so as to determine its confidence interval (Wu et al., 2020; Zhong et al., 2007). Therefore, through 10000 self-developing sampling of the existing measured data and calculating the average value of each sampling, a set composed of several mean values can be obtained, according to which the confidence interval of the evaluation index can be obtained. If the index value is in the 95% confidence interval corresponding to the index, it determines the high-quality of the measured data, which is marked as 1. If the index value is outside the 95% confidence interval, the measured data is judged as low-quality data by the index, which is marked as 0. At the same time, when the quality of the measured data is labeled, the peak trend is obvious, and the high synchronization of the SO_2 and CO_2 average series is considered as high-quality data, and the quality label is 1; if the two series have large differences and drastic changes occur frequently, they are considered as low-quality data, and the quality label is 0. Combined with the evaluation results of indexes and quality labels, the evaluation accuracy of each index is calculated, and a certain number of indexes with high accuracy are selected to form an index set to jointly evaluate the data quality. The distance between the index value of the measured data and overall mean of the central position of the confidence interval is calculated, and the ratio to the unilateral length of the confidence interval is obtained. The closer the ratio is to 0, the better the quality of the measured data. On the contrary, the closer to 1 means the worse the quality of the measured data. When the

https://doi.org/10.5194/acp-2022-452
Preprint. Discussion started: 12 July 2022


Atmospheric Chemistry and Physics Discussions

numerator in the ratio is greater than the denominator, the ratio is greater than 1, and the index value is not in the 95% confidence interval. Therefore, the result with a ratio greater than 1 is also reassigned to 1. In joint evaluation, if the calculated ratio of all indexes is 1, the quality of the measured data is judged to be poor, otherwise the mean value of all ratios less than 1 is closer to 0, indicating a better quality of the measured data.

4 Experiment

4.1 Data

Our research team designed and developed a sniffer system using an unmanned aerial vehicle (UAV) in the "Shanghai Free Trade Zone ship exhaust Monitoring" (MISEE) project. Field tests have demonstrated that it has the advantages of high monitoring accuracy and convenience (Zhou et al., 2019; Zhou et al., 2020). In this study, this system is used to collect SO_2 and CO_2 data of ship emissions. The monitoring site is located at Waigaoqiao Port in Shanghai, which is only 20 km from the city center. Exhaust gas measurement data (SO_2+CO_2) of 148 ships were collected between 2019 and 2021. Six groups of measurement data are defined to show the rationality and accuracy of the integral interval length selection, peak point matching and measurement data quality evaluation method. The six groups of data are 2019-9-27C, 2019-10-17C, 2021-1-13B, 2021-3-10A, 2021-8-18C, and 2021-9-3A. The date in the number is the date on which the measured data is collected in the field, and the letter indicates the group of data collected on that date. Among them, the data quality of 2021-1-13B and 2021-3-10A is better, with a strong synchronization between the two sequences, while the quality of other measured data is poor, reflecting the peak trend that SO_2 and CO_2 sequences cannot keep synchronization.

4.2 Selection of integral interval length

The result of calculating the optimal integral interval length of 148 groups of measurement data using the method discussed in 3.1 is shown in Figure 1. The standard deviation of the peak density corresponding to 12 s is the maximum, that is, 12 s is the optimal integral interval length. Therefore, the measured value per second is replaced with the average of 12 s, and the average sequence is obtained.

https://doi.org/10.5194/acp-2022-452
Preprint. Discussion started: 12 July 2022

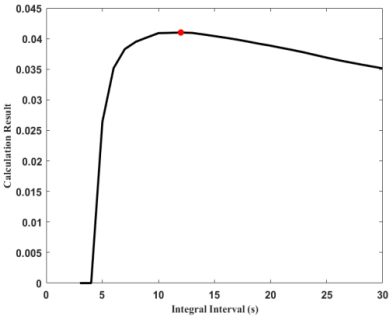

Figure 1. The 3–30 s integral interval length of the peak density standard deviation of the calculated results. The red point is the result of the calculation corresponding to the length of the 12 s integral interval, taking the maximum value.

There are differences in the quality of measurement data. High-quality measurement data have a clear peak trend, low-quality measurement data are mixed with small fluctuations, and the peak trend is not obvious. In order to verify the effect of using 12 s as the integral interval, the six groups of measurement data in Figure 2 are taken as an example, which are the measurement data numbered 2019-9-27C, 2019-10-17C, 2021-1-13B, 2021-3-10A, 2021-8-18C, and 2021-9-3A, the abscissa represents the time point, and the interval between the two points, or sampling rate, is 1 s. In addition, the data quality is indicated in the chart title, in which 2021-1-13B and 2021-3-10A are high-quality data, 2019-9-27C, 2019-10-17C, 2021-8-18C, and 2021-9-3A are low-quality data, the left side is the original measurement sequence, and the right side is the average sequence processed with the 12 s integral interval. The changing trends of SO_2 and CO_2 in 2021-1-13B and 2021-3-10A measurement data are basically synchronized. When SO_2 reaches the peak point, CO_2 will also reach the peak point in the subsequent time. The peak points at 175 formed by small fluctuations, then 210 time points in 2021-1-13B measurement data are integrated into a larger peak trend after being converted into an average series. In the 2021-3-10A measurement data, there was a sharp mutation at the 150–165, 190–210, and 300–320 time points of the SO_2 sequence, which changed to a moderate upward and downward trend after processing. At the same time, the platform values at 130, 165, 210, and 265 time points were also converted into peak points that could establish a matching relationship. There are many abrupt changes in the SO_2 sequence of 2019-9-27C measurement data, in which the peak trend at the 260 time point becomes more obvious after being replaced by the average, which can be selected as the global optimal peak. There is no obvious synchronous change in the SO_2 and CO_2 average series in 2019-10-17C, 2021-8-18C, and 2021-9-3A

https://doi.org/10.5194/acp-2022-452
Preprint. Discussion started: 12 July 2022

Atmospheric Chemistry and Physics Discussions

measurement data. The average 2019-10-17C sequence can smooth small fluctuations to some extent, and it can also transform the steep peak trend formed by drastic changes in 1750–1950 time points into a relatively gentle trend. The SO_2 sequence of 2021-8-18C only has two peak trends at 400, 475 time points, but because these two peak trends are abrupt, which are converted to average values and flattened into platform values, and there is almost no synchronization between the two sequences, it is impossible for this group of low-quality measurement data to select the global optimal peak points. Although 2021-9-3A has undergone a drastic change, the frequency of the change is not high compared with 2019-10-17C, hence the effect of the average sequence is more obvious. There are many platform values in the original CO_2 measurement series, such as those in the 0–45 and 52–90 time points. The average sequence converts all these platform values into non-platform values, which makes the overall change trend clearer.

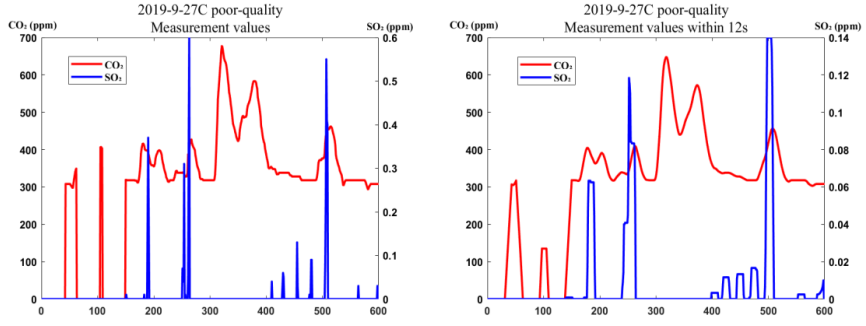

(a)

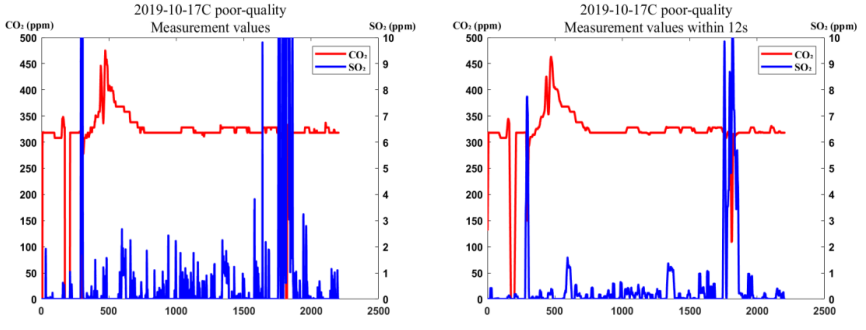

(b)

https://doi.org/10.5194/acp-2022-452
Preprint. Discussion started: 12 July 2022

Atmospheric Chemistry and Physics Discussions

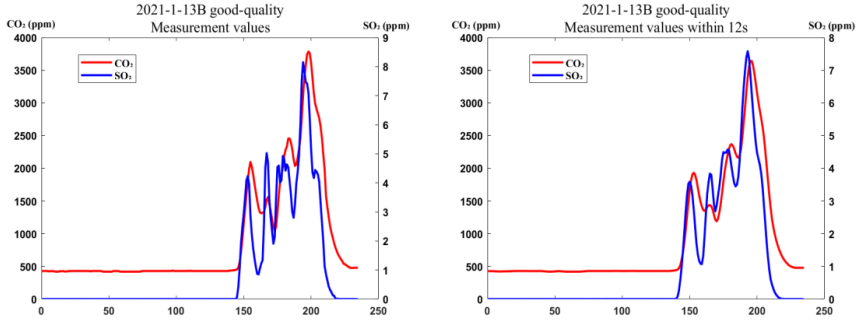

(c)

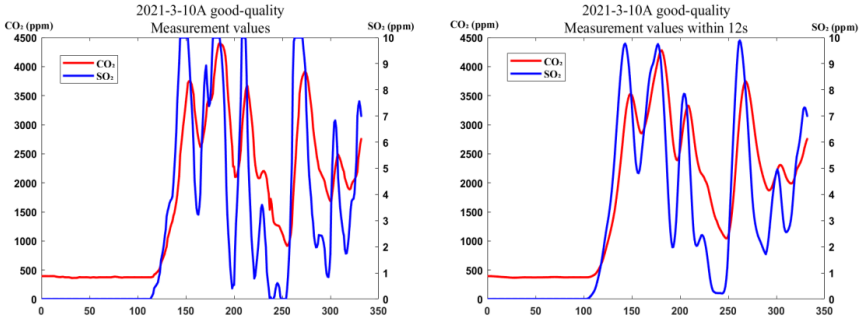

(d)

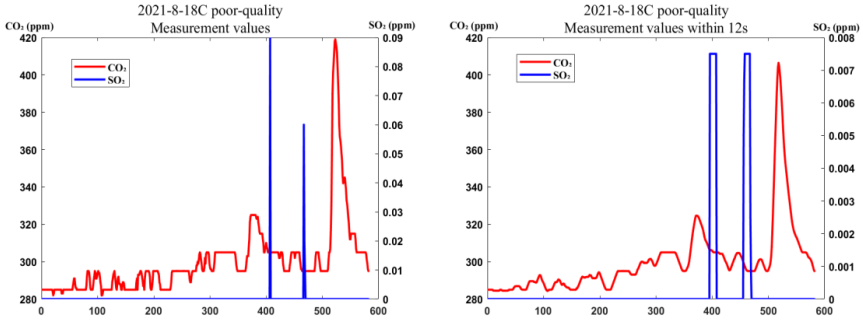

(e)

https://doi.org/10.5194/acp-2022-452
Preprint. Discussion started: 12 July 2022

Atmospheric Chemistry and Physics Discussions

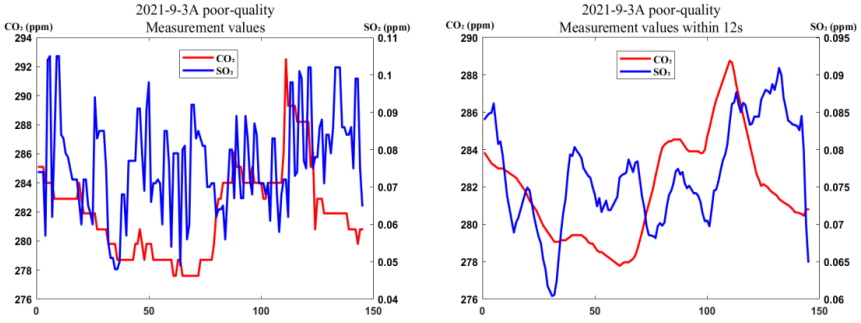

(f)

Figure 2. Groups of measurement data of SO_2 and CO_2. (a) 2019-9-27C; (b) 2019-10-17C; (c) 2021-1-13B; (d) 2021-3-10A; (e) 2021-8-18C; and (f) 2021-9-3A. The time and quality of data measurement are marked in the title. On the left is the unprocessed sequence of measurements, and on the right is the average sequence processed with the length of the 12s integral interval.

4.3 Matching of peak points and screening of global optimal peak points

After the measured value series is converted into an average series, and the peak points of SO_2 and CO_2 are extracted, the corrected time series is transformed into a matching relationship between the peak points of the two average series, and the corresponding peak point of each peak point in another series is found. The DTW algorithm based on the improved Manhattan distance is used to match the peak points of SO_2 and CO_2.

After the peak point matching is complete, the matching results with a time span of more than 20 s and drastic changes need to be eliminated. To find the threshold to distinguish between normal and abnormal changes, calculations are needed. For this reason, we use 148 sets of measurement data for DTW matching, obtain 911 matching results, calculate the difference between the normalized results of SO_2 and CO_2 in each matching result, and then use the K-means clustering algorithm for the 911 differences. The clustering result is shown in Figure 3, the result of multiple clustering is stable, and the threshold is 0.3485. Therefore, after the DTW matching for the peak points of a group of measured data, traversing all the matching results, if the normalized difference between SO_2 and CO_2 is more than 0.3485 or the time span is more than 20 s, cannot be regarded as the global optimal peak point and needs to be eliminated. The matching result containing the maximum average value of SO_2 is found among the reserved matching results, and the matching result containing the maximum average value of CO_2 is selected as the global optimal peak point from all the matching results found.

https://doi.org/10.5194/acp-2022-452
Preprint. Discussion started: 12 July 2022

Atmospheric Chemistry and Physics Discussions

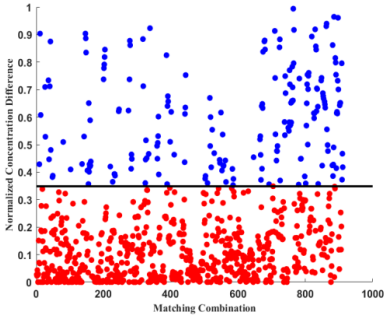

Figure 3. K-means clustering of 911 normalized differences. The red mark point refers to the normalized difference of the normal change, the blue mark point refers to the normalized difference of the abnormal change, and the black line is the threshold to distinguish normal from abnormal changes.

The results of peak point matching show that the improved Manhattan distance can consider the important time span and concentration difference. Figure 4 shows the results of three groups of measurement data (2019-9-27C, 2021-1-13B, and 2021-3-10A) screening peak points using Euclidean distance and improved Manhattan distance in the DTW algorithm. The Abscissa represents the time point, and the interval between the two points, or sampling rate, is 1 s. The reasonable global optimal peak point (in the green circle) cannot be found by using the Euclidean distance in 2019-9-27C and 2021-3-10A. The quality of 2019-9-27C is poor, the variation trend of SO_2 and CO_2 average series is different, and the platform value cannot be used as peak point at the 500 time point. The quality of 2021-3-10A data is good, but the matching relationship between SO_2 and CO_2 peak point of synchronous change at the 145, 165, and 260 time points are not established, and the normalized concentration of SO_2 in the selected global optimal peak point is lower than that of the 260 time point. The reason is that the Euclidean distance only uses the concentration difference to represent the distance of the peak point, and the matching will be given priority when there are other peak points with similar concentration near a peak. The constraint of the warping path leads to the possibility that it can no longer match the later more suitable peak points. The improved Manhattan distance can ensure that the peak points are matched preferentially with similar time span and concentration. The 2019-9-27C and 2021-3-10A groups successfully establish a correct matching relationship between the above peak points when matching using the improved Manhattan distance. As a result, the appropriate global optimal peak point is found. The SO_2 and CO_2 of the 2021-1-13B measurement data show a trend of almost synchronous change with a peak, hence both the Euclidean distance and the improved Manhattan distance give the appropriate

https://doi.org/10.5194/acp-2022-452
Preprint. Discussion started: 12 July 2022

Atmospheric Chemistry and Physics Discussions

494 global optimal peak. However, the Euclidean distance does not establish a matching relationship between
495 the peak points of this group at the 170 time point, whereas the improved Manhattan distance achieves
496 this.
497 Figure 5 shows three groups of measurements with typical problems (2019-10-17C, 2021-8-18C, 2021-
498 9-3A). There is almost no synchronous change interval between the two time-series of the 2019-10-17C
499 measurement data, and the peak trend is not clear. When using the screening algorithm, some peak points
500 with matching relationship are still retained after the time span is more than 20 s and the concentration
501 difference is more than 0.3485, but these matching results cannot be used as global optimal peak points.
502 The SO_2 measurement data in 2021-8-18C have two platform-like data (data points in the pink circle),
503 and there is no peak point of SO_2, so the global optimal peak point cannot be selected. There are 20 peak
504 points in the SO_2 sequence in 2021-9-3A and only two peak points in the CO_2 sequence. Due to the large
505 difference between the number of peak points, the warping path is easy to shift to the boundary of the
506 distance matrix, and the global optimal peak point (the peak point in the green circle) cannot establish a
507 matching relationship. For 2019-10-17C, the screening algorithm gives the global optimal peak point,
508 but the result is obviously not a suitable global optimal peak point, which is contrary to the subjective
509 judgment. For 2021-8-18C, the screening algorithm does not recognize a global optimal peak point,
510 which is consistent with the subjective judgment. For 2021-9-3A, the screening algorithm also recognizes
511 no global optimal peak point, but it is contrary to the subjective judgment.

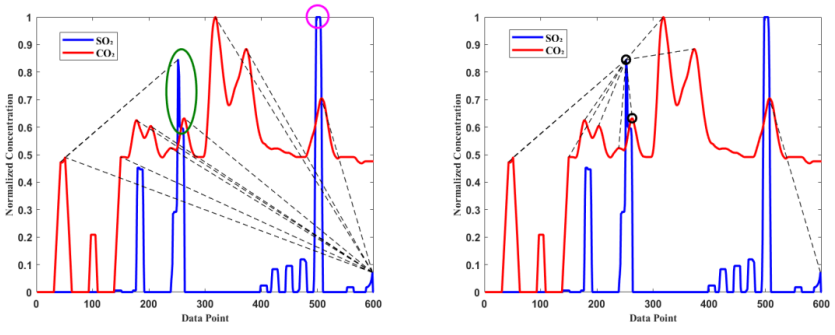

512 (a)

https://doi.org/10.5194/acp-2022-452
Preprint. Discussion started: 12 July 2022

Atmospheric Chemistry and Physics Discussions

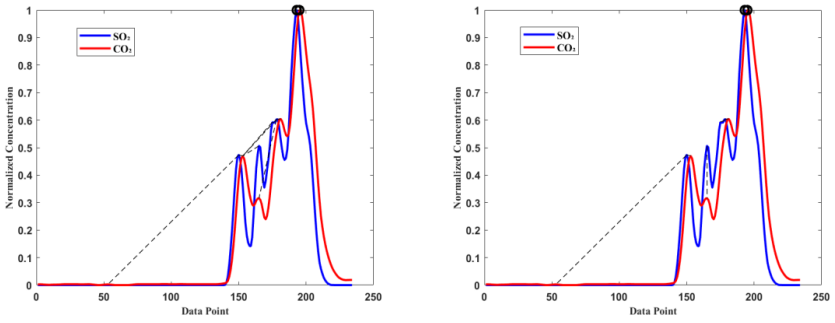

(b)

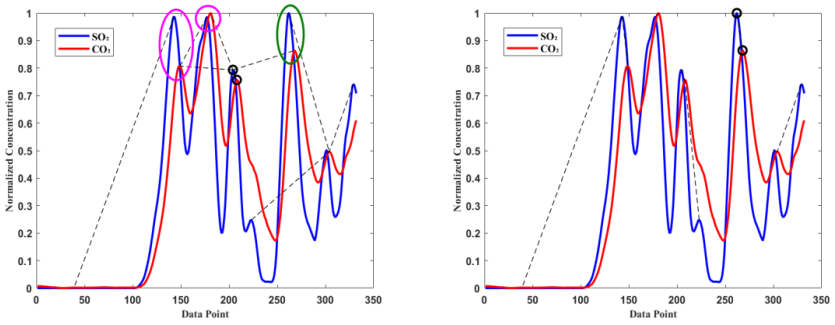

(c)

Figure 4. Four groups of measurement data of SO_2 and CO_2. (a) 2019-9-27C; (b) 2021-1-13B; and (c) 2021-3-10A. The left panels are the global optimal peak point screening result using the Euclidean distance, while the right are the global optimal peak point screening using the improved Manhattan distance. The black line is the matching relationship between the two points, the small black circle is the global optimal peak point given by the screening algorithm, the pink circle is the peak points that cannot be regarded as the global optimal peak points, and the green circle is the appropriate global optimal peak points.

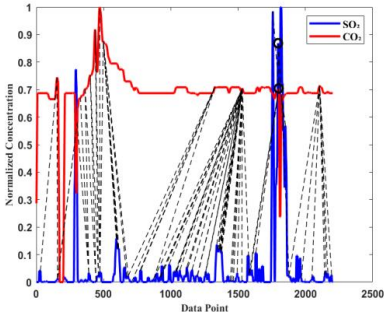

(a)

https://doi.org/10.5194/acp-2022-452
Preprint. Discussion started: 12 July 2022

Atmospheric Chemistry and Physics Discussions

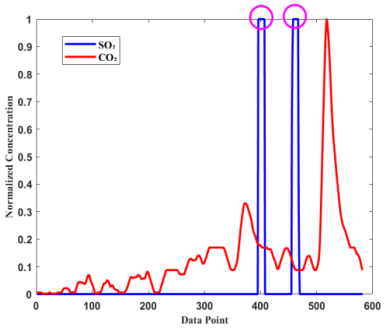

(b)

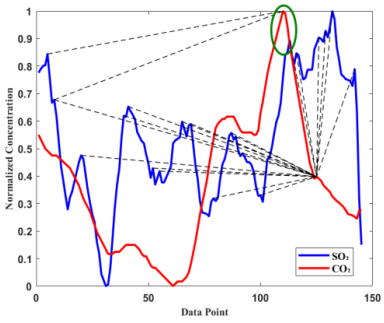

(c)

Figure 5. Three groups of SO_2 and CO_2 measurement data. (a) 2019-10-17C, (b) 2021-8-18C, and (c) 2021-9-3A. Abscissa is the point of time, and the interval between the two points, or sampling rate, is 1 s. The black line shows that there is a matching relationship between the two connected peak points, the pink circle is the peak points that cannot be regarded as the global optimal peak points, the green circle is the appropriate global optimal peak points, and the small black circle is the global optimal peak point given by the screening algorithm.

Of the 148 groups of measurement data screened, 101 groups, in which the artificial screening results are consistent with the algorithm screening, demonstrate the global optimal peak points. Among the remaining data, 19 groups of measurement data show inconsistent results, while 28 groups have poor quality that neither screening could find the global optimal peak points. Regardless of whether the global optimal peak point exists or not, the result of the algorithm is defined as correct when the results of the subjective and algorithm screenings are the same, in this case the correct rate of the screening algorithm is 87.16%. The results of the screening algorithm are consistent with the subjective screening results, but the global optimal peak points are not found, or the large deviation of time series leads to no reasonable

https://doi.org/10.5194/acp-2022-452
Preprint. Discussion started: 12 July 2022

Atmospheric Chemistry and Physics Discussions

retention of peaks in the screening matching relationship. For this measurement data, the algorithm can identify and provide the reason. There are mainly two cases of inconsistent measurement data, one is that the data can artificially screen the global optimal peak, yet the algorithm does not give the optimal result or directly determines that there is no suitable global optimal peak, the other is that there is no global optimal peak point in the data, and the result given by the algorithm is only a group of peak points where the concentration difference and time span do not exceed the threshold. The first case usually occurs in the measurement data with a large gap in the number of peak points in the average sequence of SO_2 and CO_2. When forming a distance matrix, this difference will cause one side of the row or column of the matrix to be much larger than the other. Limited by the directional constraints of the DTW algorithm, there is no other choice for the warping path to reach the matrix boundary, but can only extend vertically or horizontally along the boundary. Therefore, the appropriate global optimal peak point will not be selected by the warping path. The second situation is more common. Multiple screening conditions are defined in the screening matching relationship, and the matching relations that do not meet the conditions will be eliminated. Although the remaining matching relations meet the conditions, they may not necessarily be the optimal peak points. This situation will occur when the algorithm selects the final value from the reserved peak value.

Table 2: Algorithm screening for groups of measurement data. "Consistent (found)" means that the result given by the algorithm is the same as that of artificial selection and can find the global optimal peak point. "Consistent (not found)" means that the two results are consistent and neither of them has found the global optimal peak point. "Inconsistent" refers to the difference between the two results. "Correct rate" refers to the ratio of the 148 groups of measurement data to the 148 groups of data with "Consistent (found)" and "Consistent (not found)" measurement data.

Consistent (found)	Consistent (not found)	Inconsistent	Correct rate
129	28	19	87.16%

4.4 Verification of data quality evaluation method

In Section 3.4, 16 indexes are proposed to evaluate the quality of the measured data. The 95% confidence interval of the evaluation index is calculated by 10000 self-development sampling of the collected data, and the results are shown in Table 3.

Table 3: Self-development sampling times of 16 evaluation indexes and the upper and lower bounds of the 95% confidence interval.

https://doi.org/10.5194/acp-2022-452
Preprint. Discussion started: 12 July 2022

Atmospheric Chemistry and Physics Discussions

Evaluation index	Self-development sampling times	Lower bound of 95% confidence interval	Upper bound of 95% confidence interval
Sample entropy (SO_2)	10000	0.082153984	0.150936086
Information entropy (SO_2)	10000	3.245317702	3.721704023
Third quartile (SO_2)	10000	0.203210727	0.280760482
Standard deviation (SO_2)	10000	0.211572244	0.22958644
Skewness (CO_2)	10000	1.027746851	1.471870163
Standard deviation of peak density (CO_2)	10000	0.040255915	0.045275922
Permutation entropy (SO_2)	10000	0.694783281	0.752033377
Fuzzy entropy (CO_2)	10000	0.179056426	0.216571182
Approximate entropy (CO_2)	10000	0.140398491	0.167099422
Mutual information	10000	0.588883766	0.647985481
First quartile (SO_2)	10000	0.042864083	0.089750709
Kurtosis (CO_2)	10000	5.435791486	7.228334146
DTW shortest distance	10000	14.44706187	26.07445393
Quartile spacing (SO_2)	10000	0.152163801	0.207432999
Coefficient of variation (SO_2)	10000	1.651178674	1.980617162
Ratio of the number of peak points	10000	1.996089804	6.083568681

The results of the 16 evaluation indexes for 148 groups of measurement data are shown in Table 4. Some indexes are selected to form the index set. Skewness (CO_2) and information entropy (SO_2) with the highest accuracy of index evaluation are taken as the elements in the initial subset. After comparing the accuracy of adding other indexes, it is found that when the elements in the index set are skewness (CO_2), information entropy (SO_2), sample entropy (SO_2), and quartile spacing (SO_2), the joint evaluation can achieve relatively good results, with a correct rate of up to 70.95%. When the index continues to increase, the correct rate decreases, indicating that these indexes can only represent part of the characteristics of the measured data and have high coupling. Therefore, these four indexes are selected for joint evaluation. The six groups of measurements in Figure 6 have all been defined. This section uses the quality evaluation method to evaluate the quality and verify the rationality of the six groups of data. The groups

https://doi.org/10.5194/acp-2022-452
Preprint. Discussion started: 12 July 2022

Atmospheric Chemistry and Physics Discussions

575 2019-9-27C, 2021-1-13B, and 2021-3-10A are the measurements that can screen out the global optimal
576 peak points, but the SO_2 and CO_2 series in 2019-9-27C do not have a synchronous trend, and only the
577 two series have the same peak trend at 2019-9-27C, thus even if they can be used as global optimal peak
578 points, the ratio of the four evaluation indexes is 1, and the joint evaluation result is poor quality. There
579 are four peak trends in 2021-1-13B, where SO_2 and CO_2 change almost synchronously. The peak trend
580 at the 200 time point is very clear and higher than other peaks, which belongs to the appropriate global
581 optimal peak point, and the result of joint evaluation of indexes is very close to 0. The peak trend in
582 2021-3-10A is slightly more than that of 2021-1-13B, although altogether is basically synchronous; the
583 peak trend at 145, 160, 260 time points can be observed, while between the global optimal peak point is
584 the priority to select the maximum value of the average SO_2. Finally, the peak point at the 260 time point
585 is selected as the global optimal peak point, and the joint evaluation result of the index is higher than that
586 of 2021-1-13B. The SO_2 average sequence of 2019-10-17C has frequent small fluctuations and abrupt
587 changes over time, and there is no obvious synchronous peak trend, while the SO_2 sequence of 2021-8-
588 18C has platform values only at 400, 480 time points, thus it cannot be used as the global optimal peak
589 point. The average series of SO_2 and CO_2 in 2021-9-3A show a synchronous change trend at 90–110 time
590 points, hence SO_2 fluctuates greatly relative to CO_2. Although the peak point at the 110 time point can
591 be selected as the global optimal peak, and the result of joint evaluation of the index remains 1. To
592 summarize, the results of the quality evaluation methods for poor and good quality data are in line with
593 expectations.

594 **Table 4: Sixteen indexes for the evaluation of 148 groups of measurement data statistics.**

Index	Number of correct evaluation results	Number of wrong evaluation results	Correct rate
Sample entropy (SO_2)	86	62	58.11%
Information entropy (SO_2)	90	58	60.81%
Third quartile (SO_2)	87	61	58.78%
Standard deviation (SO_2)	86	62	58.11%
Skewness (CO_2)	91	57	61.49%
Standard deviation of peak density (CO_2)	82	66	55.41%

https://doi.org/10.5194/acp-2022-452
Preprint. Discussion started: 12 July 2022

Atmospheric Chemistry and Physics Discussions

Permutation entropy (SO_2)	81	67	54.73%
Fuzzy entropy (CO_2)	82	66	55.41%
Approximate entropy (CO_2)	87	61	58.78%
Mutual information	76	72	51.35%
First quartile (SO_2)	82	66	55.41%
Kurtosis (CO_2)	85	63	57.43%
DTW shortest distance	73	75	49.32%
Quartile spacing (SO_2)	88	60	59.46%
Coefficient of variation (SO_2)	87	61	58.78%
Ratio of the number of peak points	74	74	50.00%

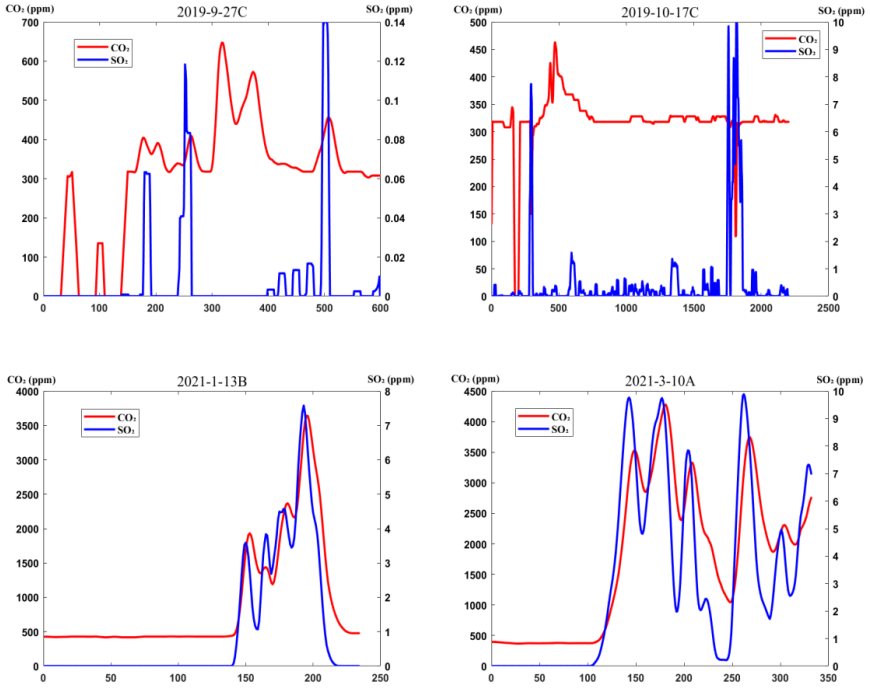

https://doi.org/10.5194/acp-2022-452
Preprint. Discussion started: 12 July 2022

Atmospheric Chemistry and Physics Discussions

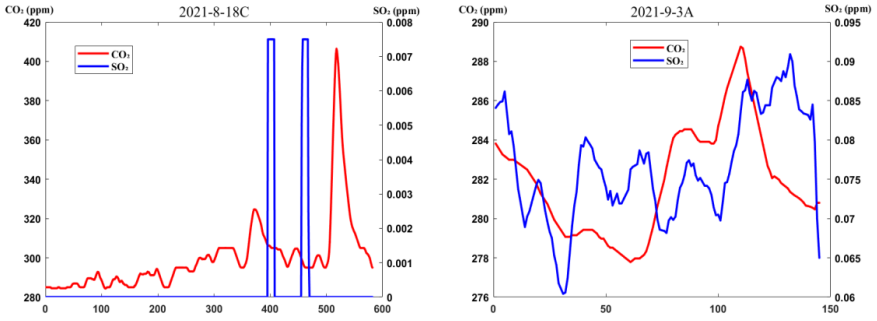

595 **Figure 6. Evaluation of the quality of the six groups of SO_2 and CO_2 measurement data. The Abscissa is the**
596 **time point, and the interval between the two points, or sampling rate, is 1s.**

597 **Table 5: Algorithm screening of six groups of measurement data (2019-9-27C, 2019-10-17C, 2021-1-13B,**
598 **2021-3-10A, 2021-8-18C, and 2021-9-3A). The specific values and evaluation results of information entropy**
599 **(SO_2), sample entropy (SO_2), skewness (CO_2), quartile spacing (SO_2) and the results of joint evaluation of the**
600 **four indexes.**

Data ID	Algorithm	Information entropy		Sample entropy		Skewness		Quartile spacing		Result of joint evaluation
		Value	EVAL	Value	EVAL	Value	EVAL	Value	EVAL	
2019-9-27C	√	1.7112	1	0.0307	1	-0.6145	1	0.0060	1	1
2019-10-17C	×	2.6154	1	0.0353	1	-3.8664	1	0.0240	1	1
2021-1-13B	√	2.6865	1	0.0272	1	1.6976	1	0.1801	0.0116	0.0116
2021-3-10A	√	5.1502	1	0.1061	0.3050	0.2466	1	0.5737	1	0.3050
2021-8-18C	√	0.3047	1	0.0076	1	3.1325	1	0	1	1
2021-9-3A	×	5.8638	1	0.7894	1	0.4692	1	0.3711	1	1

601 **"×" indicates that the screening algorithm is inconsistent with subjective judgment**

602 **5 Conclusion**

603 The emission factor is an important parameter for compiling ship emission inventory. Various studies
604 have measured emission factors under different conditions. However, there is little attention and research
605 on improving the accuracy, confidence, and automation of the calculation methods.
606 In this study, we propose a high accuracy calculation of ship emission factors and an evaluation of the

https://doi.org/10.5194/acp-2022-452
Preprint. Discussion started: 12 July 2022


Atmospheric Chemistry and Physics Discussions

quality of measurement data based on the sniffer method. Altogether, we optimize the calculation process, select the appropriate integral interval length to convert the original measurement data into an average value to make the calculation results more stable, and put forward the concept of peak density standard deviation selection for the optimal integral interval length, which reduces the uncertainty caused by the use of empirical values. The average sequence is extracted to find all the peak points, and the matching relationship with the measured series of SO_2 and CO_2 is found by using the DTW algorithm based on the improved Manhattan distance. The unreasonable matching results are eliminated according to the concentration change and time span thresholds analyzed. The maximum concentration of SO_2 and CO_2 in the remaining matching relationship is the global optimal peak point. In order to evaluate the quality of the measured data objectively, 16 evaluation indexes, which can reflect the characteristics of the measured data are selected, and the 95% confidence interval of each index is calculated by self-expanding sampling of the measured data, and combined with the quality label of the measured data. Several indexes with high accuracy of data quality evaluation are selected to jointly evaluate the measured data, further optimizing the accuracy of the evaluation.

We used 148 groups of sniffer measurements collected between 2019 and 2021 to test the rationality of the above methods. When the length of the integral interval is 12 s, the standard deviation of peak density reaches the maximum. Compared with the change trend of several groups of data before and after preprocessing, the peak trend of the data set after preprocessing is more obvious, and most of the nonsignificant trends in the series are smoothed out. Comparing the artificial and algorithm screening results of the global optimal peak points of 148 groups of measured data, 129 groups have the same results, with a correct rate of 87.16%. After 10000 times of self-development sampling, the 16 evaluation indexes all reached the 95% confidence interval. When using four evaluation indexes: information entropy (SO_2), sample entropy (SO_2), quartile spacing (SO_2), and skewness (CO_2), 70.95% of the data quality labels are consistent with the joint evaluation results of the evaluation index set. When using these four indexes to quantify data quality, it is consistent with expectations, which verifies that the data quality evaluation method is feasible.

The emission factor calculation and measurement data quality evaluation methods proposed in this study can reduce the uncertainty in the current sniffer technique monitoring ship emission research, objectively evaluate the measurement data quality, and provide data support for the accurate establishment of an emission inventory. Future work is needed to further analyze the characteristics of the measured data so

https://doi.org/10.5194/acp-2022-452
Preprint. Discussion started: 12 July 2022

Atmospheric Chemistry and Physics Discussions

as to improve the global optimal peak point screening algorithm. At the same time, it is also necessary to find other evaluation indexes that can reflect the characteristics of the measured data to reduce the coupling in the evaluation index set, improve the accuracy of the joint evaluation index set and quantification of the quality of the data.

Data availability

Please address requests for data sets and materials to Fan Zhou (fanzhou_cv@163.com).

Author contribution

LZ analyzed the experimental data and authored the article. FZ designed the study and provided constructive comments on this research.

Competing interests

The authors declare that they have no conflict of interest.

Acknowledgements

This research was supported by the National Natural Science Foundation of China (grant No. 41701523) and Science and Technology Commission of Shanghai Municipality (grant No. 22692107400), as well as the Shanghai High-level Local University Innovation Team (Maritime Safety & Technical Support).

References

Balzani Lööv, J. M., Alfoldy, B., Gast, L. F. L., Hjorth, J., Lagler, F., Mellqvist, J., Beecken, J., Berg, N., Duyzer, J., Westrate, H., Swart, D. P. J., Berkhout, A. J. C., Jalkanen, J. -P., P -rata, A. J., van der Hoff, G. R., and Borowiak, A.: Field test of available methods to meas -ure remotely SO_x and NO_x emissions from ships, Atmos. Meas. Tech., 7, 2597-2613, https://doi.org/10.5194/amt-7-2597-2014, 2014.

Beecken, J., Mellqvist, J., Salo, K., Ekholm, J., and Jalkanen, J. -P.: Airborne emission measur -ements of SO_2, NO_x and particles from individual ships using a sniffer technique, Atmos. Meas. Tech., 7, 1957-1968, https://doi.org/10.5194/amt-7-1957-2014, 2014.

Burgard, D. A., and Bria, C. R. M.: Bridge-based sensing of NO_x and SO_2 emissions from ocean-going ships, Atmos. Environ., 136, 54-60, https://doi.org/10.1016/j.atmosenv.2016.04.014, 2016.

Betha, R., Russell, L. M., Sanchez, K. J., Liu, J., Price, D. J., Lamjiri, M. A., Chen, C. L., K -uang, X. M., da Rocha, G. O., Paulson, S. E., Miller, J. W., and Cocker, D. R.: Lower N-O_x but Higher Particle and Black Carbon Emissions from Renewable Diesel compared to Ult -ra Low Sulfur Diesel in At-Sea Operations of a Research Vessel, Aerosol. Sci. Tech., 51, 123-134, https://doi.org/10.1080/02786826.2016.1238034, 2017.

Bai, C. J., Li, Y., Liu, B. X., Zhang, Z. Y., and Wu, P.: Gaseous Emissions from a Seagoing Ship under Different Operating Conditions in the Coastal Region of China, Atmosphere-Basel., 11, 305, https://doi.org/10.3390/atmos11030305, 2020.

https://doi.org/10.5194/acp-2022-452
Preprint. Discussion started: 12 July 2022

672 Corbett, J. J., and Fischbeck, P.: Emissions from ships, Science., 278, 823-824, https://doi.org/1
673 0.1126/science.278.5339.823, 1997.
674 Cooper, D. A.: Exhaust emissions from ships at berth, Atmos. Environ., 37, 3817-3830, https://
675 doi.org/10.1016/S1352-2310(03)00446-1, 2003.
676 Chen, D. S., Zhang, Y., Lang, J. L., Zhou, Y., Li, Y., Guo, X. R., Wang, W. L., and Liu, B.:
677 Evaluation of different control measures in 2014 to mitigate the impact of ship emissions on
678 air quality in the Pearl River Delta, China, Atmos. Environ., 216, 116911, https://doi.org/10.
679 1016/j.atmosenv.2019.116911, 2019.
680 Dmytrów, K., Landmesser, J., and Bieszk-Stolorz, B.: The Connections between COVID-19 and
681 the Energy Commodities Prices: Evidence through the Dynamic Time Warping Method, Ene
682 -rgies., 14, 4024, https://doi.org/10.3390/en14134024, 2021.
683 Ekmekçioğlu, A., Kuzu, S. L., Ünlügençoğlu, k., and Çelebi, U. B.: Assessment of shipping e-
684 mission factors through monitoring and modelling studies, Sci. Total. Environ., 743, 140742,
685 https://doi.org/10.1016/j.scitotenv.2020.140742, 2020.
686 Huang, J. R., and Xiang, Y. J.: The Application of the Remote Monitoring System for Ship E-
687 xhaust Gas of Bridge Foundation in the Supervision of Marine Fuel Oil in the Estuary Wate
688 -rs, Journal of Guangzhou Maritime Institute., 29, 26-30, https://doi.org/10.3969/j.issn.1009-85
689 26.2021.04.006, 2021.
690 Hu, J. B., Zhu, J. H., Peng, S. T., Zhao, H. X., and Hong, N. N.: Sniffing method: a techniq-
691 ue to estimate sulfur content in marine fuel through in situ measurements of ship emissions,
692 Journal of Waterway and Harbor, 39, 619-625, https://doi.org/10.3969/j.issn.1005-8443.2018.05.
693 015, 2018.
694 Itakura, F.: Minimum prediction residual principle applied to speech recognition, IEEE Transacti
695 -ons on Acoustics, Speech, and Signal Processing, 23, 67-72, https://doi.org/10.1109/TASSP.19
696 75.1162641, 1975.
697 Jonson, J. E., Gauss, M., Schulz, M., Jalkanen, J. P., and Fagerli, H.: Effects of global ship e-
698 missions on European air pollution levels, Atmos. Chem. Phys., 20, 11399-11422, https://doi.
699 org/10.5194/acp-20-11399-2020, 2020.
700 Kesgin, U., and Vardar, N.: A study on exhaust gas emissions from ships in Turkish Straits, A
701 -tmos. Environ., 35, 1863-1870, https://doi.org/10.1016/S1352-2310(00)00487-8, 2001.
702 Liu, H., Fu, M. L., J, X. X., Shang, Y., Shindell, D., Faluvegi, G., Shindell, C., and He, K.
703 B.: Health and climate impacts of ocean-going vessels in East Asia, Nat. Clim. Change., 6,
704 1037-1041, https://doi.org/10.1038/nclimate3083, 2016.
705 Liu, Y. S., Ge, Y. S., Tan, J. W., Fu, M. L., Shah, A. N., Li, L. Q., Ji, Z., and Ding, Y.: Em
706 -ission characteristics of offshore fishing ships in the Yellow Bo Sea, China, J. Environ. Sci.
707 , 65, 83-91, https://doi.org/10.1016/j.jes.2017.02.020, 2018.
708 Li, H. H., Liu, J. X., Yang, Z. L., Liu, R. W., Wu, K. F., and Wan, Y.: Adaptively constraine
709 -d dynamic time warping for time series classification and clustering, Inform. Sciences., 534,
710 97-116, https://doi.org/10.1016/j.ins.2020.04.009, 2020.
711 Matthias, V., Bewersdorff, I., Aulinger, A., and Quante, M.: The contribution of ship emissions
712 to air pollution in the North Sea regions, Environ. Pollut., 158, 2241-2250, https://doi.org/10.
713 1016/j.envpol.2010.02.013, 2010.
714 Moreno-Gutiérrez, J., Calderay, F., Saborido, N., Boile, M., Valero, R. R., and Durán-Grados,
715 V.: Methodologies for estimating shipping emissions and energy consumption: A comparative

https://doi.org/10.5194/acp-2022-452
Preprint. Discussion started: 12 July 2022

analysis of current methods, Energy., 86, 603-616, https://doi.org/10.1016/j.energy.2015.04.083, 2015.

Mohajan, H. K.: Acid Rain is a Local Environment Pollution but Global Concern, J. Anal. Ch -em+., 3, 47-55, https://mpra.ub.uni-muenchen.de/id/eprint/91622, 2018.

Papaefthimiou, S., Maragkogianni, A., and Andriosopoulos, K.: Evaluation of cruise ships emiss -ions in the Mediterranean basin: The case of Greek ports, Int. J. Sustain. Transp., 10, 985-9 94, https://doi.org/10.1080/15568318.2016.1185484, 2016.

Peng, Z. H., Ge, Y. S., Tan, J. W., Fu, M. L., Wang, X., Chen, M., Yin, H., and Ji, Z.: Emis -sions from several in-use ships tested by portable emission measurement system, Ocean. En- g., 116, 260-267, https://doi.org/10.1016/j.oceaneng.2016.02.035, 2016.

Sinha, P., Hobbs, P. V., Yokelson, R. J., Christian, T. J., Kirchstetter, T. W., and Bruintjes, R.: Emissions of trace gases and particles from two ships in the southern Atlantic Ocean, Atmos , Environ., 37, 2139-2148, https://doi.org/10.1016/S1352-2310(03)00080-3, 2003.

Sofiev, M., Winebrake, J. J., Johansson, L., Carr, E. W., Prank, M., Soares, J., Vira, J., Kouzn -etsov, R., Jalkanen, J. P., and Corbett, J. J.: Cleaner fuels for ships provide public health b- enefits with climate tradeoffs, Nat. Commun., 9, 406, https://doi.org/10.1038/s41467-017-0277 4-9, 2018.

Tichavska, M., and Tovar, B.: Port-city exhaust emission model: An application to cruise and f -erry operations in Las Palmas Port, Transport. Res. A-Pol., 78, 347-360, https://doi.org/10.10 16/j.tra.2015.05.021, 2015.

Toscano, D., Murena, F., Quaranta, F., and Mocerino, L.: Assessment of the impact of ship em -issions on air quality based on a complete annual emission inventory using AIS data for th- e port of Naples, Ocean. Eng., 232, 109166, https://doi.org/10.1016/j.oceaneng.2021.109166, 2 021.

UNCTAD: Review of Maritime Transport 2021, available at: https://unctad.org/webflyer/review-maritime-transport-2021, last access: 10 June 2022.

Wu, Y. Q., Huang, Z. J., Zhang, Z. W., Zhang, L. H., Wang, Y. L., Xie, Y., Wang, Y. R., an- d Zheng, J. Y.: Influence of ship emissions and its uncertainty on air quality in China, Chin -a. Environ. Science., 40, 2870-2879, https://doi.org/10.19674/j.cnki.issn1000-6923.2020.0320, 2 020.

Yang, L., Zhang, Q. J., Zhang, Y. J., Lv, Z. Y., Wang, Y. N., Wu, L., Feng, X., and Mao, H. J.: An AIS-based emission inventory and the impact on air quality in Tianjin port based on localized emission factors, Sci. Total. Environ., 783, 146869, https://doi.org/10.1016/j.scitotenv. 2021.146869, 2021.

Zhong, L. J., Zheng, J. Y., Lei, G. Q., and Chen, J.: Quantitative Uncertainty Analysis in Air Pollutant Emission Inventories: Methodology and Case Study, Res. Environ. Sciences., 20, 15 -20, https://doi.org/10.13198/j.res.2007.04.19.zhonglj/004, 2007.

Zhang, F., Chen, Y. J., Tian, C. G., Lou, D. M., Li, J., Zhang, and G., Matthias, V.: Emission factors for gaseous and particulate pollutants from offshore diesel engine vessels in China, Atmos. Chem. Phys., 16, 6319-6334, https://doi.org/10.5194/acp-16-6319-2016, 2016.

Zhang, Y., Gu, J., Wang, W., Peng, Y. Q., Wu, X. J., and Feng, X. J.: Inland port vessel emi- ssions inventory based on Ship Traffic Emission Assessment Model-Automatic Identification System, Adv. Mech. Eng., 9, 1-9, https://doi.org/10.1177/1687814017712878, 2017.

Zhang, Y., Yang, X., Brown, R., Yang, L., Morawska, L., Ristovski, Z., Fu, Q., and Huang, C.

https://doi.org/10.5194/acp-2022-452
Preprint. Discussion started: 12 July 2022

Atmospheric Chemistry and Physics Discussions

760 : Shipping emissions and their impacts on air quality in China, Sci. Total. Environ., 581-582
761 , 186-198, https://doi.org/10.1016/j.scitotenv.2016.12.098, 2017.
762 Zhou, F., Pan, S. D., Chen, W., Ni, X. P., and An, B. W.: Monitoring of compliance with fuel
763 sulfur content regulations through unmanned aerial vehicle (UAV) measurements of ship emi
764 -ssions, Atmos. Meas. Tech., 12, 6113-6124, https://doi.org/10.5194/amt-12-6113-2019, 2019.
765 Zhou, F., Gu, J., Chen, W., and Ni, X. P.: Measurement of SO_2 and NO_2 in Ship Plumes Usi-
766 ng Rotary Unmanned Aerial System, Atmosphere-Basel., 10, 657, https://doi.org/10.3390/atmo
767 s10110657, 2019.
768 Zhou, F., Hou, L. W., Zhong, R., Chen, W., Ni, X. P., Pan, S. D., Zhao, M., and An, B. W.:
769 Monitoring the compliance of sailing ships with fuel sulfur content regulations using unman-
770 ed aerial vehicle (UAV) measurements of ship emissions in open water, Atmos. Meas. Tech.,
771 13, 4899-4909, https://doi.org/10.5194/amt-13-4899-2020, 2020.